Contribution from the Institut für Organische Chemie und Lehrstuhl für Theoretische Chemie der Universität Heidelberg,
D-6900 Heidelberg, West Germany, Anorganisch-Chemisches Institut der
Technischen Universität München, D-8046 Garching, West Germany, and Institut für Anorganische Chemie der Universität
Erlangen-Nürnberg, D-8520 Erlangen, West Germany

Electronic Structure of the P_3, As_3, and Sb_3 Units in a Nortricyclane Skeleton

ROLF GLEITER,*[†] HORST KÖPPEL,[‡] PETER HOFMANN,[§] HELMUT R. SCHMIDT,[§]
and JOCHEN ELLERMANN[∥]

Received December 18, 1984

The He I photoelectron (PE) spectra of the three cage compounds **1**–**3** have been recorded. The assignment of the first five bands in the PE spectra is based on model calculations (MINDO/3), correlation with related species, and a band shape analysis of the first two bands. It is concluded that the highest occupied MO's of all three compounds are the e and a_1 linear combinations of the lone pairs centered at the X_3 unit. The shape of the first two bands in the PE spectra can be attributed to a combined action of Jahn–Teller and spin–orbit coupling in the ionic ground state.

Introduction

Recently the P_3, As_3, and, to a lesser extent, the Sb_3 units have been discovered to be building blocks in a number of cage structures with the nortricyclane skeleton. Examples are P_4S_3, As_4S_3, P_7Li_3, and $P_4[Si(CH)_3)_2]_3$. These species are of interest due to their optical and electrical properties,[1] their spectral behavior,[2] their reactivity toward acceptors,[3] and their potential as building blocks for larger units.[4] With the synthesis of the cage compound 4-methyl-1,2,6-triphosphatricyclo[2.2.1.0^{2,6}]heptane (**1**) and its arsa (**2**) and stiba (**3**) analogues,[5,6] nearly ideal models have become available for the study of bonding properties prevailing in the X_3 unit with C_{3v} symmetry. In this paper we report investigations of **1**–**3** using He I photoelectron (PE) spectroscopy and model calculations.

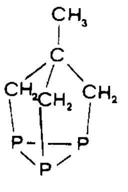
1

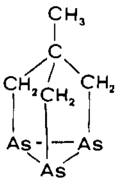
2

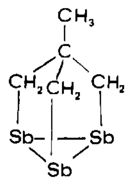
3

PE Spectra of 1–3

The PE spectra of **1**–**3** are shown in Figure 1. The vertical ionization energies, $I_{v,j}$, are collected in Table I. The PE spectra of **1**–**3** are similar in so far as they show two bands (bands 1 and 2) at low energy, well separated from a single one (band 3) followed by two more intense and broad bands (bands 4 and 5) each representing at least two electronic configurations of the ion. The first two bands overlap strongly in the phosphorus compound **1** while in its As and Sb congeners, **2** and **3**, both bands are clearly separated and relatively sharp. We will deal with these striking differences in the series **1**–**3** further below.

In order to interpret the PE spectra we will proceed in two ways: we will compare the experimental results with appropriate model calculations and will try to correlate the PE bands with those of related compounds.

Calculations

A correlation between the measured vertical ionization energies, $I_{v,j}$, and calculated orbital energies, ϵ_j, is possible via Koopmans' theorem, which states that the negative value of the orbital energy can be set equal to the vertical ionization energy ($-\epsilon_j = I_{v,j}$).[7] This approximation implies that the wave functions obtained for the ground state can also be used to describe the different ionic states. Usually Koopmans' approximation can be used for the outer valence electrons by using canonical MO's.

Since reliable parameters for As and Sb are not available, we use the P compound as a model. In Table II the calculated orbital energies for the highest occupied MO's for **1** are listed by using the MINDO/3 method[8] with the P parameters suggested by Frenking et al.[9] Together with the orbital energies, we also list the type of the wave functions along with their composition. The three highest occupied MO's are strongly localized at the P centers. They can be described as the three linear combinations arising from the lone pairs on the phosphorus atoms. Figure 2 shows contour diagrams of one component of the 7e MO and of $7a_1$ plotted in the *x,y* plane, 0.35 Å below the P_3 triangle (left), and in the *x,z* plane bisecting **1** containing the exocyclic C–C bond and one C–P bond (right). The following two MO's, 6e, are about equally localized on the P_3 unit and the carbon skeleton and can be described as Walsh type orbitals centered at the P_3 unit heavily mixed with 2p type orbitals at the C skeleton. The MO belonging to the irreducible representations 5e is localized in the C–X as well as in the C–C and the C–H bonds, while $6a_1$ is mainly localized in the C–X bonds (see Table II).

Table I. Vertical Ionization Energies (eV) of **1**–**3**

compd	$I_{v,1}$	$I_{v,2}$	$I_{v,3}$	$I_{v,4}$	$I_{v,5}$
1	8.6	8.8	9.9	10.2	11.5
2	8.40	8.63	9.4	9.8	10.9
3	7.70	8.08	8.63	9.1	9.8

Table II. Calculated Orbital Energies and Wave Functions (MINDO/3) for **1** (C_{3v})[a]

$-\epsilon_j$, eV	Γ^b	% P	% C	MO type
8.84	7e	86	4	lone pair
9.06	$7a_1$	80	17	lone pair
9.95	6e	40	47	Walsh
10.71	5e	21	52	C–P, C–C, C–H σ
11.16	$6a_1$	40	50	C–P

[a] Full geometry optimization of **1** within the MINDO/3 frame yields a C_{3v} structure with the following relevant structural parameters: P–P = 221.7 pm, P–C = 195.7 pm, C_{CH_2}–C = 160.9 pm, C–C_{CH_3} = 151.9 pm; angle P–P–C = 92.4°, P–C_{CH_2}–C = 110.72°, C_{CH_2}–C–C_{CH_3} = 115.70°; the CH_3 group is staggered with respect to the cage skeleton. [b] Only the valence electrons are counted.

[†] Institut für Organische Chemie der Universität Heidelberg.
[‡] Lehrstuhl für Theoretische Chemie der Universität Heidelberg.
[§] Anorganisch-Chemisches Institut der Technischen Universität München.
[∥] Institut für Anorganische Chemie der Universität Erlangen-Nürnberg.

(1) Salanek, W. R.; Liang, K. S.; Paton, A.; Lipari, N. O. *Phys. Rev. B: Solid State* **1975**, *12*, 725.
(2) Baudler, M.; Tennberger, H.; Faber, W.; Hahn, J. *Z. Naturforsch., B: Anorg. Chem., Org. Chem.* **1979**, *34B*, 1690.
(3) Cordes, A. W.; Joyner, R. D.; Shores, R. D.; Dill, E. D. *Inorg. Chem.* **1974**, *13*, 132. Fritz, G.; Uhlmann, R. *Z. Anorg. Allg. Chem.* **1980**, *465*, 59.
(4) Baudler, M. *Angew. Chem.* **1982**, *94*; 520; *Angew. Chem., Int. Ed. Engl.* **1982**, *21*, 492. von Schnering, H. G. In "Homoatomic Rings, Chains and Macromolecules of Main Group Elements"; Rheingold, A. L., Ed.; Elsevier: Amsterdam 1977; p 317. von Schnering, H. G. *Angew. Chem.* **1981**, *93*, 44; *Angew. Chem., Int. Ed. Engl.* **1981**, *20*, 33.
(5) Ellermann, J.; Schössner, H. *Angew. Chem.* **1974**, *86*, 646; *Angew. Chem., Int. Ed. Engl.* **1974**, *13*, 601. Thiele, G.; Zoubek, G.; Lindner, H. A.; Ellermann, J. *Angew. Chem.* **1978**, *90*, 133; *Angew. Chem., Int. Ed. Engl.* **1978**, *17*, 135.
(6) Ellermann, J.; Veit, A. *Angew. Chem.* **1982**, *94*, 377; *Angew. Chem., Int. Ed. Engl.* **1982**, *21*, 375. Ellermann, J.; Demuth, A. A. M. *Angew. Chem.* **1984**, *96*, 785; *Angew. Chem., Int. Ed. Engl.* **1984**, *23*, 805.
(7) Koopmans, T. *Physica* (*Amsterdam*) **1934**, *1*, 104.
(8) Bingham, R. C.; Dewar, M. J. S.; Lo, D. H. *J. Am. Chem. Soc.* **1975**, *97*, 1285.
(9) Frenking, G.; Goetz, H.; Marschner, F. *J. Am. Chem. Soc.* **1978**, *100*, 5295.
(10) Weast, R. E., Ed. "Handbook of Chemistry and Physics"; CRC Press: Boca Raton, FL, 1980.

0020-1669/85/1324-4020$01.50/0

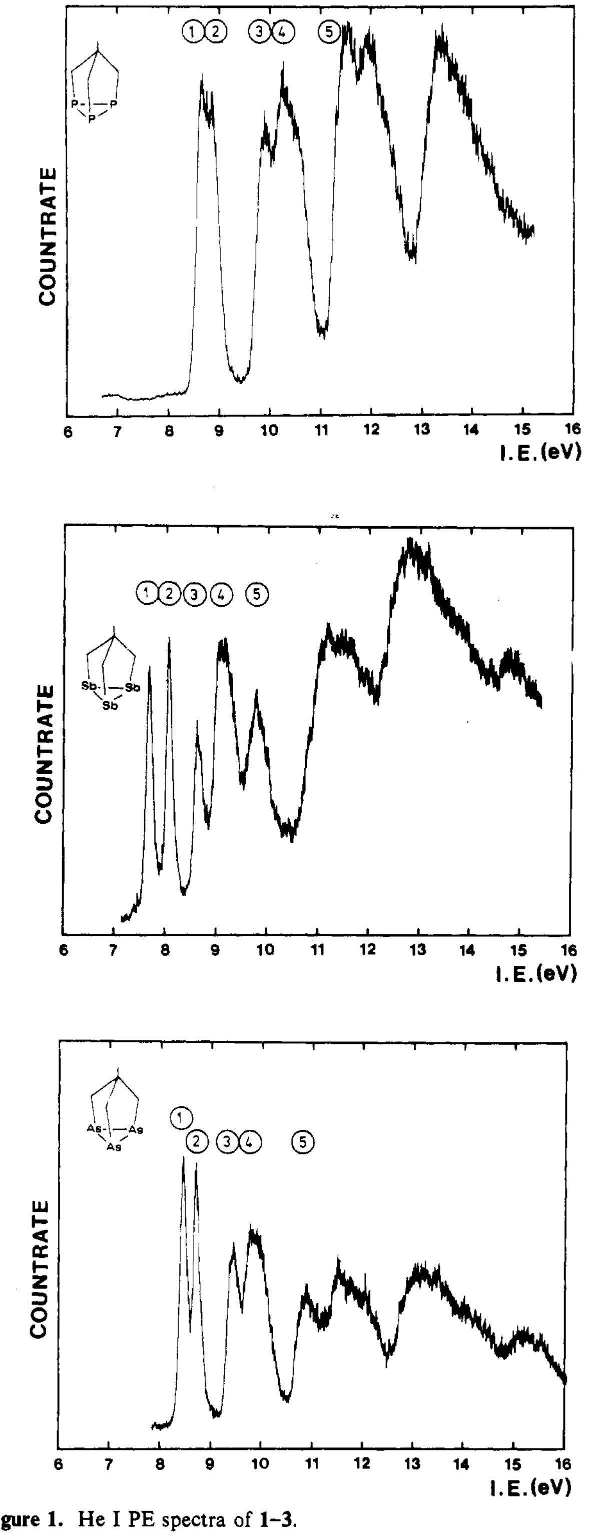

Figure 1. He I PE spectra of **1**–**3**.

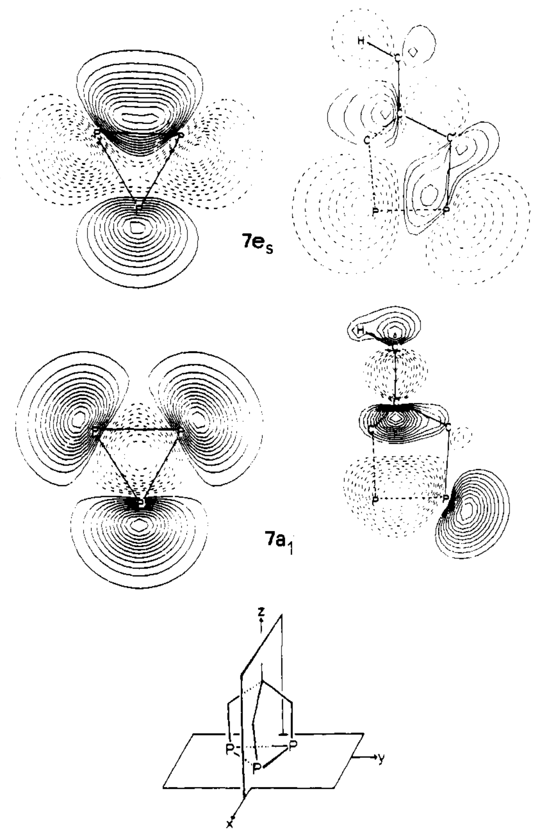

Figure 2. Wave function contour diagrams of the highest occupied MO's of **1** according to a MINDO/3 calculation. The contours are drawn in the x,y plane, 0.35 Å below the P_3 unit, and in the x,z plane bisecting **1** containing the exocyclic C–C and one C–P bond.

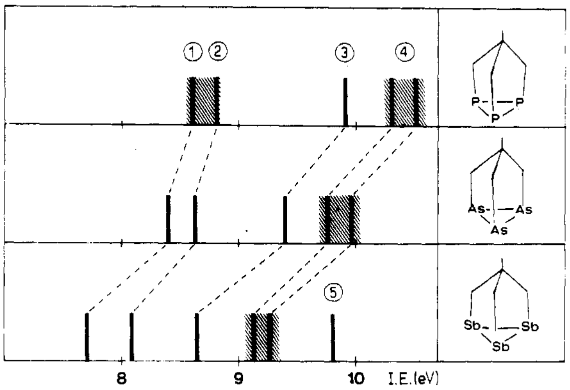

Figure 3. Correlation between the first five bands of the PE spectra of **1**–**3**.

Assignment and Correlations

On the basis of previous work,[11-14] one expects for **1**–**3** orbitals of the following type as highest occupied molecular orbitals: lone pairs on the heteroatoms X (e, a), followed by X–X σ-bonds (Walsh type e, a), C–X σ-bonds (a and e), and finally C–C and C–H σ-bonds. In line with this qualitative reasoning are the results of MINDO/3[8,9] calculations on **1** (Table II). A comparison with these results and the PE spectrum of **1** suggests an assignment of bands 1 and 2 to ionizations from 7e, band 3 to $7a_1$, and band 4 to ejections from 6e. To confirm this assignment we have compared in Figure 3 the first bands of the PE spectra of **1** with those of **2** and **3**. We observe a relatively small shift between the first two bands in the PE spectra of **1** and those of **2** while the shift between the first two bands of **2** and those of **3** is found to be similar to that observed for bands 3 and 4 for **1**–**2** and **2**–**3**. Since the two highest occupied MO's are strongly localized within the X_3 unit, the observed difference in the shift of the corresponding bands might be traced back to the difference in the first ionization energies of X (P 10.5 eV, As 9.8 eV, and Sb 8.6 eV).[10] In line with this rationalization is the observation that the energy difference between the first band in the PE spectra of simple alkyl derivatives $(CH_3)_nX(CF_3)_{3-n}$ (n = 1–3, X = P, As, Sb)[11] is found to be smaller for the P–As series compared with As–Sb compounds. Similarly a small energy difference is also encountered by comparing the first five bands of the PE spectra of $P_3(t\text{-}Bu)_3$

---

(11) Elbel, S.; Bergmann, H.; Ensslin, W. *J. Chem. Soc., Faraday Trans. 2* **1974**, 555. Gleiter, R.; Goodman, W. O.; Schäfer, W.; Grobe, J.; Apel, J. *Chem. Ber.* **1983**, *116*, 3745.

(12) Gleiter, R.; Böhm, M. C.; Baudler, M. *Chem. Ber.* **1981**, *114*, 1004.

(13) Gleiter, R.; Schäfer, W.; Baudler, M. *J. Am. Chem. Soc.*, in press.

(14) Gleiter, R.; Böhm, M. C.; Eckert-Maksić, M.; Schäfer, W.; Baudler, M.; Aktalay, Y.; Fritz, G.; Hoppe, K.-D. *Chem.Ber.* **1983**, *116*, 2972.

(**4**)[12] with those of $As_3(t\text{-}Bu)_3$ (**5**).[13] For band 5 in the spectra of **1**–**3** the assignment is less certain. In the case of **1** an assignment to 5e and perhaps $6a_1$ seems reasonable if we use intensity criteria. The wave functions of both MO's can be described as C–X σ-bonds with mixing of C–H and C–C σ-bonds (see Table II). A comparison between the energies of band 5 in the series **1**–**3** shows a shift similar to that of bands 1–4 (see Table I); this argues for a relatively strong participation of the heteroelement in the corresponding wave function, and it is suggested to assign band 5 in the PE spectra of **2** and **3** to $6a_1$ only. Intensity criteria support this idea.

A comparison between the recorded ionization energies (Table I) and the calculated orbital energies (Table II) of **1** gives reasonable agreement with the exception of $7a_1$ (band 3). $7a_1$ is predicted to lie at too low an energy. This discrepancy might be rationalized as due to $^2E(E_{1/2})$–$^2A(E_{1/2})$ coupling. Since the ^2A ionized state also transforms as $E_{1/2}$, both $^2E(E_{1/2})$ and $^2A(E_{1/2})$ will interact and thus lead to an additional separation of both bands.

The relatively strong shift toward lower ionization energies of bands 3 and 4 in **2** and **3** with respect to **1** might be due to an increase of the inductive effect of the X_3 unit with respect to the carbon skeleton.

A further corroboration of our assignment of the PE spectrum of **1** is given by the comparison of the centers of gravity of the first five bands of the PE spectra of **1** (9.8 eV) with those of **4** (9.0 eV). The corresponding comparison **2**–**5** yields 9.4 eV for **2** and 8.8 eV for **5**. Due to the larger carbon skeleton in **4** and **5** the center of gravity of the first five bands is shifted by 0.6–0.8 eV as anticipated.

The sequence of MO's of **1** parallels those obtained for $P_4[Si(CH_3)_2]_3$ (**6**),[14] with the difference that in **6** the delocalization of the highest occupied MO's is stronger than in **1**. This can be rationalized by the assumption that the basis orbital energies of the carbon skeleton and the P_3 unit are more apart in energy than the corresponding fragments in **6**.

For a future comparison of the reactivity of **1**–**3** and **6** with that of other nortricyclane-structured cages like $P_7(CH_3)_3$ (**7**), $P_7[Si(CH_3)_3]_3$ (**8**), P_4S_3 (**9**), and As_4S_3 (**10**), it is interesting to note that the highest occupied MO's of **7**–**10** are mainly localized on the equatorial centers of the cage as evidenced by calculations and PE investigations on **7**–**10**.[14–16]

Band Shape Considerations

As pointed out above, the shape of the first two bands as well as their energy difference changes considerably (see Figure 1).

There are two well-known mechanisms that may lead to a splitting of a band for ionization out of a degenerate MO, the Jahn–Teller effect[17] and spin–orbit coupling.[18] Spin–orbit coupling will certainly be of relevance for **3** and also **2**, because of the heavy atoms forming the basal ring (Sb and As, respectively). However, it can hardly be the only mechanism responsible for the splitting, because its observed increase 0.20:0.23:0.38 = 0.53:0.61:1.00 in the series **1**–**3** is much weaker than expected from the strong dependence of the spin–orbit splitting on the atomic charge Z. In the case of a first-order spin-orbit coupling this would lead to an increase[19] like $Z^2(P):Z^2(As):Z^2(Sb) = 15^2:33^2:51^2 = 0.087:0.42:1.00$ in the series **1**–**3**. Also, in the P compound **1** spin–orbit coupling alone cannot account for the magnitude of the observed splitting of 0.2 eV. We therefore attempt to explain the splitting and shape of the composite bands in question by the combined action of the Jahn–Teller (JT) effect and of spin–orbit (SO) coupling.

To make this idea more precise, we restrict our attention to the basal X_3 ring, where the e MO's are localized, and use the following model Hamiltonian for the nuclear motion under the simultaneous influence of JT and SO coupling:[20]

$$\mathcal{H} = \begin{vmatrix} H_0 + \lambda/2 & \kappa(x + iy) \\ \kappa(x - iy) & H_0 - \lambda/2 \end{vmatrix} \qquad (1a)$$

$$H_0 = T_N + (\omega/2)(x^2 + y^2) + E \qquad (1b)$$

The different rows and columns of the two by two matrix (1a) refer to the two complex components of the ^2E ionic state. x and y are dimensionless coordinates of the JT active vibration of the X_3 ring and are related to the displacements Q_x and Q_y defined in eq 2.[21] In this equation f stands for the force constant for the

$$u = (fM/\hbar^2)^{1/4}Q_u \qquad u = x, y \qquad (2)$$

JT active vibration and M for its effective mass. In (1b) T_N stands for the kinetic energy of this mode, $\omega = \hbar\ (f/M)^{1/2}$ for its frequency (in energy units), and E for the vertical ionization potential (energy of the band center[22]). Thus, the operator H_0 describes the unperturbed vibrational motion. The JT and SO couplings are represented by the terms κ and λ, respectively.

According to eq 1 the shape of the first PE bands is governed by the three parameters ω, κ, and λ. In principle, those could be determined for each of the compounds **1**–**3** by a least-squares fit of the spectrum corresponding to eq 1 to the experimental recording. However, the described agreement with experiment becomes more significant, and more insight into the structural features of the coupling mechanism is gained, if we can reproduce the observations with an *universal* set of parameters for the series **1**–**3**. It has already been mentioned that in the case of a first-order effect the SO splitting is proportional to Z^2 to a good approximation. In X_3 ring systems, on the other hand, first-order SO coupling is not exclusively operative, but will be accompanied by second-order SO coupling,[23] the latter arising from nondiagonal elements of the SO operator (especially with the nearby ionic state with a hole in the $7a_1$ orbital). By perturbation theoretic arguments this contribution to the SO splitting is expected to be roughly proportional to Z^4. For the sake of simplicity, and to avoid the variation of too many parameters, we will, however, ignore the second-order contribution to the SO splitting in the numerical calculations and take the latter to be proportional to Z^2. The significance of this simple approximation will be discussed below.

To obtain a similar scaling law for the JT coupling constant κ and the frequency ω, we assume that the potential energy surfaces in the absence of SO coupling are *independent* of Z. This implies that ω and κ depend on the specific molecule only via its effective mass M of vibration (see eq 2). Since M is proportional to the mass M_x of the basal X atoms, we can write

$$\lambda = \lambda_0 Z^2 \qquad (3)$$

$$\kappa = \kappa_0/(M_x)^{1/4} \qquad (4)$$

$$\omega = \omega_0/(M_x)^{1/2} \qquad (5)$$

To determine the universal parameters λ_0, κ_0, and ω_0, we proceed in two steps. First we focus on the magnitude ΔE of the separation of the two band maxima. For a spectrum described by the Hamiltonian (1), ΔE is well approximated by eq 6.[24] With the

$$\Delta E = (\pi\kappa^2 + \lambda^2)^{1/2} \qquad (6)$$

aid of eq 3 and 4 we can fix λ_0 and κ_0 by requiring that for any

---

(15) Bock, H.; Solouki, B.; Fritz, G.; Hölderich, N. *Z. Anorg. Allg. Chem.* **1979**, *458*, 53.

(16) Head, J. D.; Mitchell, K. A. R.; Noodleman, L.; Paddock, N. L. *Can. J. Chem.* **1977**, *55*, 669. Cannington, P. H.; Whitfield, H. J. *J. Electron Spectr. Relat. Phenom.* **1977**, *10*, 35.

(17) See, for example: Bersuker, I. B. "The Jahn-Teller Effect and Vibronic Interactions in Modern Chemistry"; Plenum Press, New York, 1984.

(18) See, for example: Richards, W. G.; Trivedi, H. P.; Cooper, D. L. "Spin-Orbit Coupling in Molecules"; Clarendon Press: Oxford, England, 1981.

(19) Heilbronner, E.; Hornung, V.; Kloster-Jensen, E. *Helv. Chim. Acta* **1970**, *53*, 331.

(20) Schenk, H. J.; Schwarz, W. H. E. *Theor. Chim. Acta* **1972**, *24*, 225.

(21) Gerber, W. H.; Schumacher, E. *J. Chem. Phys.* **1978**, *69*, 1692.

(22) Cederbaum, L. S.; Domcke, W. *J. Chem. Phys.* **1976**, *64*, 603.

(23) Manne, R.; Wittel, K.; Molanty, B. S. *Mol. Phys.* **1975**, *29*, 485.

(24) Habitz, P.; Schwarz, W. H. E. *Theor. Chim. Acta* **1973**, *28*, 267. Our eq 6 differs from eq 1 of Habitz and Schwarz by a factor of $\pi/2$, which derives from a Franck–Condon analysis of the spectral moments (Köppel, H. Dissertation, TU München, 1979) and which has been found to lead to a better agreement with exact numerical calculations.

Table III. Jahn–Teller and Spin–Orbit Parameters for the Species **1**–**3** Used in Figure 4[a]

compd	atom	Z	M	λ	κ	ω
1	P	15	31	0.030	0.126	0.020
2	As	33	75	0.145	0.101	0.013
3	Sb	51	122	0.345	0.089	0.010

[a] λ, κ, and ω are given in eV.

two compounds of the series **1**–**3** the observed split is reproduced by eq 6. The As and Sb compounds **2** and **3** have been selected to that end, and with the resulting data we have calculated ΔE for the P compound **1**. The result of this simple calculation (0.23 eV) compares nicely with the observed ΔE (0.20 eV), which is an encouraging indication for the applicability of our approach.

As a second step we have performed full dynamical calculations of the vibronic structure of the first PE bands, using the Hamiltonian (1). (For the method of calculation see ref 25). The results of step 1 for λ_0 and κ_0 have been adopted without change, and ω_0 has been determined by requiring that the observed band envelope of the P compound **1** be well reproduced. The parameter values thus deduced are collected in Table III, and the first PE bands of **1**–**3** calculated with these data are displayed in Figure 4.

Comparing these curves with those of Figure 1, we see that the main features of the experimental recordings are well reproduced by the calculation. Not only the magnitude of the splitting but also the depth of the central dip and the asymmetry of the two maxima for **1**–**3** are given correctly by the Hamiltonian (1).

We conclude that the characteristic shape of the first PE bands and the change in the series **1**–**3** are grasped correctly by our simple model and can indeed be attributed to the combined action of Jahn–Teller and spin–orbit coupling in the ionic ground states. As a byproduct this model calculation also confirms the assignment of the first bands to ionization out of the 7e MO. An inspection of Table III reveals that in the Sb compound **3** the split ΔE is dominated by SO coupling, while in the P compound **1** it is caused almost exclusively by JT coupling; in the case of **2** both couplings contribute to a comparable extent to it. The decrease of the JT coupling constant κ with increasing M explains why the ΔE increases much slower in the series **1**–**3** than on grounds of the SO coupling alone.

At this point a word of caution seems appropriate concerning the precise values of the parameters given in Table III. As already mentioned above, the SO splitting in our series of compounds cannot be strictly proportional to Z^2 as was assumed in eq 3. Therefore, the numerical values of Table III cannot be quantitatively reliable. More realistic is probably a form of λ as a sum of Z^2 and Z^4 terms that represent the first-order and second-order contributions to the SO splitting, respectively. We have also performed a few calculations where the SO splitting was taken to be proportional to Z^4. These calculations gave invariably too large a split of the band maxima in **1** compared to that in **2** and **3**. For this reason we believe that the Z^2 (or first-order) contribution to the SO splitting dominates in these compounds and that the above analysis, which neglected the second-order contributions, is at least qualitatively correct.

We finally comment on the geometric distortion of the cationic ground states induced by the Jahn–Teller effect. This can be found by searching for the minimum of the lower potential energy corresponding to the Hamiltonian $\mathcal{H}$, eq 1. A simple calculation[25] gives ($\rho = (x^2 + y^2)^{1/2}$)

$$\rho_0 = \left(\frac{\kappa^2}{\omega^2} - \frac{\lambda^2}{4\kappa^2}\right)^{1/2} \qquad (7)$$

provided the expression under the square root sign is positive (otherwise $\rho_0 = 0$). A nonzero value of ρ_0 means that the basal X_3 triangle of **1**, **2**, or **3** is distorted from its equilateral form in the ground state of the neutral molecule to an obtuse- or acute-angled isoceles triangle in its ionic ground state. From eq 7 we see that the spin–orbit coupling leads to a decrease of ρ_0 and thus counteracts the Jahn–Teller effect as far as the distortion of the molecular framework is concerned. Inserting the parameter values of Table III, one finds nevertheless that ρ_0 is nonzero in all three compounds and that it even increases in the series **1**–**3**. This means that the molecular distortion is dominated in *all* three cases by the Jahn–Teller effect and that the spin–orbit coupling has only a very minor influence in this respect. Of course, it would be interesting to check this prediction of our simple model calculations by a more direct experimental investigation such as an ESR experiment. Within the PE experiment, the distortion has a distinct consequence for the line structure which is, however, not resolved experimentally: according to the calculation (see Figure 4) the first peak of the band envelope is always characterized by a strong excitation of the JT-active vibration. According to the Franck–Condon principle,[26] this just reflects the change in molecular geometry occurring upon ionization.

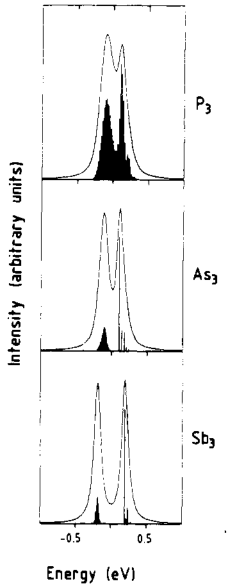

Figure 4. First PE bands of **1**–**3** as calculated with the Hamiltonian (1) and the parameter values of Table III. The energy E of the band center has been arbitrarily put to zero in all cases. The envelopes are drawn by convoluting the line spectra with Lorentzians of width fwhm = 0.1 eV. This width is somewhat larger than the nominal spectrometer resolution and is taken to include broadening effects, which may arise from rotational excitation or from excitation of other vibrational modes, not considered in the JT calculation.

Experimental Section

The preparation of **1**–**3** has been reported elsewhere.[5,6] The PE spectra of **1**–**3** have been recorded on a PS 18 spectrometer (Perkin-Elmer) and on a UPS instrument (Leybold Heraeus) and calibrated with reference to the argon and xenon lines. A resolution of 0.02 eV has been obtained on the sharp peaks. The recording temperatures were as follows: **1**, 60 °C; **2**, 85 °C; **3**, 135 °C.

Acknowledgment. We are grateful to the Deutsche Forschungsgemeinschaft, the Fonds der Chemischen Industrie, and the BASF Aktiengesellschaft, Ludwigshafen, for financial support. We thank A. Roth and A. Flatow for recording the PE spectra. The preparation of samples of **1**–**3** by A. A. M. Demuth and Drs. H. A. Lindner and A. Veit is also gratefully acknowledged.

Registry No. **1**, 92366-00-2; **2**, 52196-03-9; **3**, 81602-63-3.

---

(25) Köppel, H.; Domcke, W.; Cederbaum, L. S. *Adv. Chem. Phys.* **1984**, *57*, 59.

(26) Herzberg, G. "Spectra of Diatomic Molecules"; Van Nostrand: New York, 1950.